Geotechnical Engineering for the Preservation of Monuments and Historic Sites III

Edited by
Renato Lancellotta, Carlo Viggiani,
Alessandro Flora, Filomena de Silva,
and Lucia Mele

CRC Press
Taylor & Francis Group

Geotechnical Engineering for the Preservation of Monuments and Historic Sites III – Lancellotta, Viggiani, Flora, de Silva & Mele (Eds)

Safeguarding of the *Aurelian Walls* at *Porta Asinaria* from conventional tunnelling

S. Rampello & L. Masini
University of Rome La Sapienza

ABSTRACT: Construction of the line C of Rome underground is being carried out in a complex context due to the presence of archaeological artefacts, historical buildings and monuments of invaluable value. Along the contract T3 of the line, between the shaft 3.3 and *San Giovanni* station, two tunnels have been excavated for a length of about 140 m following a three step procedure: excavation of two small diameter tunnels with a mini TBM; soil improvement via low-pressure cement grouting; and conventional excavation of the two line tunnels in the improved soil. The tunnels, excavated at a depth of about 25 m, reach *San Giovanni* station passing at a short distance from the ancient Aurelian Walls. This paper presents the displacement measured at ground surface during the construction activities, showing the efficiency of a protective barrier made by a line of piles in reducing the movements induced by tunnelling in the Aurelian Walls.

1 INTRODUCTION

The construction of new underground railway lines and the extension of existing ones require deep open excavations and bored tunnels in urban environments, in close vicinity to existing buildings and structures. In these conditions, the main design requirement is to contain ground movements during and after the excavation works to prevent nearby structures from undergoing excessive deformations. This is particularly relevant for existing structures of monumental and historical value for which the limits in allowable movements are very onerous, as it often the case in European cities.

Contract T3 of the new line C of the Rome underground, currently under construction, underpasses the historical centre of the city encountering the historical monuments of Roman age (I to V century): these are the Aurelian Walls at *Porta Asinaria* and *Porta Metronia*, the Church of *Santo Stefano Rotondo*, the *Acquedotto Celimontano*, the *Anfiteatro Flavio* (Coliseum), the *Basilica di Massenzio*, the *Colonnacce* and the *Foro di Cesare*.

Due to the exceptional archaeological and historical value of the structures potentially affected by the construction of the line, the design included a detailed study of the interaction between the construction activities and the monuments. To this aim, the general contractor, Metro C, set-up a multidisciplinary steering technical committee with the assignment of implementing all the necessary procedures to safeguard the monuments and historical buildings.

The main tasks of the steering committee were: (i) to evaluate the influence of the construction of the line C (tunnelling and deep open excavations) on the existing monuments; (ii) to suggest, where necessary, appropriate geotechnical or structural mitigation measures; (iii) to develop a comprehensive and redundant monitoring scheme to follow in real time the response of the monuments to construction; (iv) to assist the general contractor during construction with the evaluation of the monitoring data, to optimise construction sequences and procedures.

The analysis of the interaction between the excavation activities and built environment was carried out following procedures of increasing complexity.

 DOI 10.1201/9781003308867-17

At a first stage, simplified (Level 1) analyses were performed computing surface and near-surface displacements by semi-empirical methods, ignoring the stiffness and weight of the existing monuments (e.g.: Attewell & Woodman 1982; Attewell et al. 1986; Ou & Hsieh 2011); evaluation of the potential damage induced by tunneling and deep excavations was carried out through the interaction diagrams proposed by Burland & Wroth (1974), which relate the deflection ratio and the horizontal tensile strain to given damage categories. Based on the outcome of these evaluations, the study ended if the damage was deemed negligible, or continued to a higher level of complexity (Level 2).

At this second stage, the interaction between the tunnels or the deep excavations and the monuments was studied through 2D or 3D Finite Element (FE) analyses that studied the soil-structure interaction adopting a simplified description of the mechanical behaviour of the monuments. Damage was then re-evaluated using the interaction diagrams. Depending on the computed results, either damage was deemed acceptable, or prospective remedial techniques were suggested (Burghignoli et al. 2013; Rampello et al. 2012).

Structural and geotechnical mitigation interventions have been adopted in the project of the line C, the first being aimed to strengthen the structures, while the second to reduce the ground movements induced by tunnelling or deep excavations.

Definitive structural interventions mainly consisted of reinforcements made by steel wire ropes, or chains made by steel bars (e.g.: Church of *Santo Stefano Rotondo* and *Basilica di Massenzio*), while temporary structural intervention manly consisted of buttresses made of steel tube-joint structures and multiprop towers (e.g.: Aurelian Walls at *Porta Asinaria* and *Porta Metronia*, and *Basilica di Massenzio*).

The geotechnical mitigation interventions were of active or passive type, the first permitting to control the ground settlements during tunnelling, while the second producing a favourable variation of the displacement field induced by tunnelling.

Compensation grouting is an example of active mitigation intervention whose efficiency has been shown by site applications (e.g.: Mair 2008; Mair & Hight 1994) and laboratory tests (e.g.: Masini et al. 2012, 2014). A protective embedded barrier is instead an example of passive mitigation intervention that can be adopted when the structure lies to the side of the tunnel: it is installed before tunnelling, between the tunnel and the structure for which damage must be prevented, providing a restraint to ground movements (e.g.: Bai et al. 2014; Bilotta, 2008; Bilotta & Taylor, 2005; Di Mariano et al. 2007; Fantera et al. 2016; Katzenbach et al. 2013; Masini & Rampello, 2021; Rampello et al. 2019).

During construction of the line C, compensation grouting was adopted to prevent potential damage induced by tunnel excavation under the Aurelian Walls at *Porta Metronia*, while an embedded barrier was preinstalled to protect the Aurelian Walls at *Porta Asinaria*. In both cases, field monitoring was carried out to verify the design assumptions and evaluate the actual performance of the excavation works, having also the opportunity of calibrating the semi-empirical methods.

This paper describes the displacement field monitored during conventional excavation of two tunnels, about 140 m long, connecting the multifunctional shaft 3.3, operating as a launch pit for the TBM/EPB machines which excavated the tunnels in the direction of *Amba Aradam* station, and the existing *San Giovanni* station. Both the shaft 3.3 and the tunnels were excavated close to the Aurelian Walls at *Porta Asinaria* (3rd century A.D.). To prevent any damage eventually induced by tunnelling on the ancient city wall, a protective barrier made by adjacent piles was preinstalled close to the North-bound tunnel, where the walls are closest to the tunnel, at 23 m to 26 m from its axis.

Field monitoring provided the surface ground movements induced by the three-step procedure adopted to construct the tunnels: (i) mechanised excavation of two mini-tunnels; (ii) soil improvement via low-pressure cement grouting; (iii) conventional excavation of the main tunnels in the improved soil.

In this paper, the reduction of the surface settlements obtained behind the barrier, in the portion of soil facing the ancient city wall, is evaluated through the comparison of the monitoring data collected in *green-field* conditions and in the presence of the barrier, demonstrating the efficiency of this kind of mitigation intervention.

2 THE AURELIAN WALLS AT PORTA ASINARIA

The Aurelian Walls are large defensive walls built by Emperor Aurelian between 270 and 275 A.D. with most of their length (12.5 km over 19 km) having survived past centuries in a fair preservation state. Aurelian Walls at *Porta Asinaria* belong to the South-Eastern part of the town wall and are located at a distance of 24 m to 27 m from the diaphragm wall of a 30 m-deep excavation and of 23 m to 34 m from the axis of the North-bound tunnel of the line C of the Rome underground. Figure 1a shows the aerial view of the Aurelian Walls at *Porta Asinaria*, together with the multifunctional pit 3.3. The latter operated as a launch pit for the two TBM/EPB machines that bored the 6.7 m-diameter twin tunnels in the direction of *Amba Aradam* station, while the two conventional tunnels, about 140m long, were excavated towards *San Giovanni* station.

The wall is 4 m thick and about 18 m tall from the foundation plane, with the foundation located at 8–9 m below ground surface. The structure of the Aurelian Walls is made of combined tuff and brick masonry, with an inner core of poorly bonded tuff blocks. Initially, the ground surface was at the same level on both sides of the walls but, over the centuries, material has been accumulated on the side facing the *Basilica di San Giovanni*. Nowadays the city wall retains a backfill of anthropic origin, about 10 m high, cumulated since medieval times without installing any drainage system, which has caused the development of outwards displacements as high as about 0.4 m at the top of the walls and diffused cracks along the masonry surface. The aerial photo of Figure 1b shows the Aurelian Walls and *Porta Asinaria* during the excavation of the multifunctional pit 3.3, together with the temporary safeguarding interventions installed against the wall façade and the back-excavation carried out to reduce the earth trust acting in the wall.

Unlike the wall, *Porta Asinaria* is characterised by the same elevation of the ground surface on both the *extra-* and the *intra-moenia* sides (Figure 1c–d). Its current state largely corresponds to the restorations of the time of the Emperor Honorius. The structure of *Porta Asinaria* is essentially composed of two semi-circular towers connected to each other by two walkways placed on two different levels. The towers today are about 25 m high from the elevation of ground surface on the *extra-moenia* side (+33.9 m asl) with a diameter of about 4.9 m, while the walkway area is about 18 m high.

Thanks to the recent restorations carried out since 1950, *Porta Asinaria* is characterised by a good state of conservation, with extensive portions of the masonry completely rebuilt. However, the restoration mainly concerned the external façade, while the core continues to have rather modest mechanical properties.

According to the FE interaction (Level 2) analyses carried out at the design stage, excavation of the multifunctional pit 3.3, as well as that of the two tunnels, would have induced not negligible effects on the walls, with an increment of wall rotation. Specifically, the numerical simulation of the shaft excavation estimated a wall rotation $\alpha = 0.11°(0.2\%)$ with a maximum settlement of the wall of 27 mm, while the numerical analysis simulating tunnels excavation, with an assumed volume loss $V_L = 2.5\%$, provided a wall rotation $\alpha = 14°$ with a maximum wall settlement of 16 mm.

The above quantities were deemed to be potentially dangerous for an already damaged ancient masonry structure. Therefore, the primary design challenge was that of preventing any damage induced by the excavation activities on the ancient and vulnerable Aurelian Walls, located a short distance away from the pit and the North-bound tunnel.

To this end, in order to attain an estimated reduction of wall rotation of about 36%: (i) about 8 m of the backfill were removed behind the wall prior to the excavation of the pit 3.3, starting from the middle plane of the shaft, located at a distance of 30 m from the Aurelian Walls, thus eliminating the earth thrust acting on it; (ii) a very stiff retaining system was designed for the shaft using 1.2 m-thick diaphragm walls, top-down construction with five levels of props made by cast-in-situ concrete stiff slabs, and a high embedment ratio of the diaphragm walls below the dredge line ($L/H = 1.56$), with the diaphragms extending in the stiff and overconsolidated Pliocene clay, thus preventing any deep-seated movement.

The monitoring data collected during shaft excavation confirmed that the back-excavation carried out to safeguards the ancient structure and the high stiffness of the support system, together with the high embedment ratio of the diaphragm walls below the dredge line, were the key to minimise the

effects induced by the excavation of the multifunctional pit on the Aurelian Wall at *Porta Asinaria* (Masini et al. 2021).

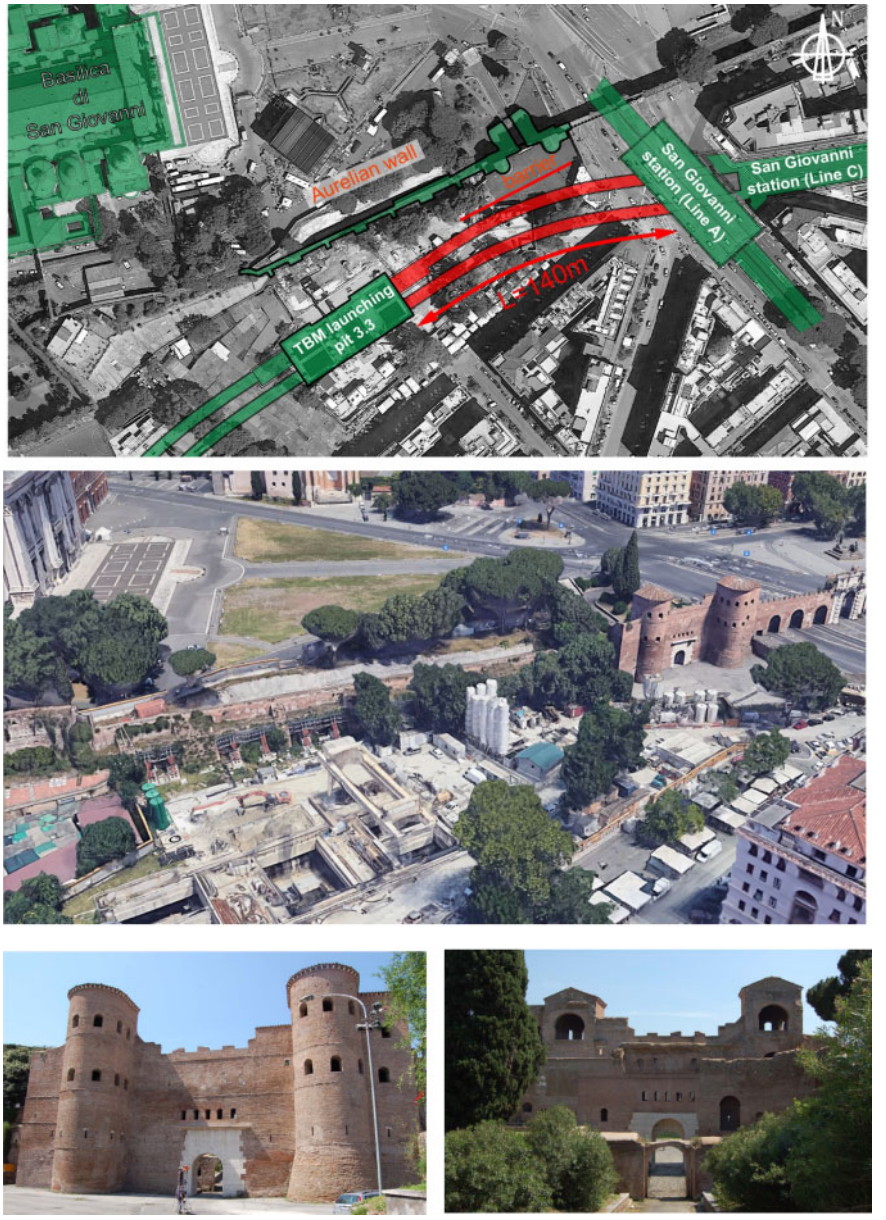

Figure 1. Aerial view of Aurelian Walls at *Porta Asinaria* (a-b); front view of *Porta Asinaria* (*extra moenia*) (c); front view of *Porta Asinaria* (*intra moenia*) (d).

To mitigate tunnelling effects, a protective barrier made by a line of piles was instead pre-installed close to the North-bound tunnel, in order to achieve an estimated reduction of about 54% in the wall rotation (see Figure 2). The efficiency of this kind of intervention, preliminary evaluated through a numerical study (Rampello et al. 2019) and a field test carried out in *green-field* conditions (Losacco et al. 2019; Masini & Rampello 2021), is discussed in this paper.

3 PROJECT DESCRIPTION AND CONSTRUCTION SEQUENCE

Figure 2 shows the two tunnels that were excavated using conventional procedures at a depth of about 25 m and for a length of 140 m, between the lunch pit 3.3 and the existing *San Giovanni* station, with the axis of the North-bound tunnel located at a distance of 23 m to 34 m from the ancient city wall.

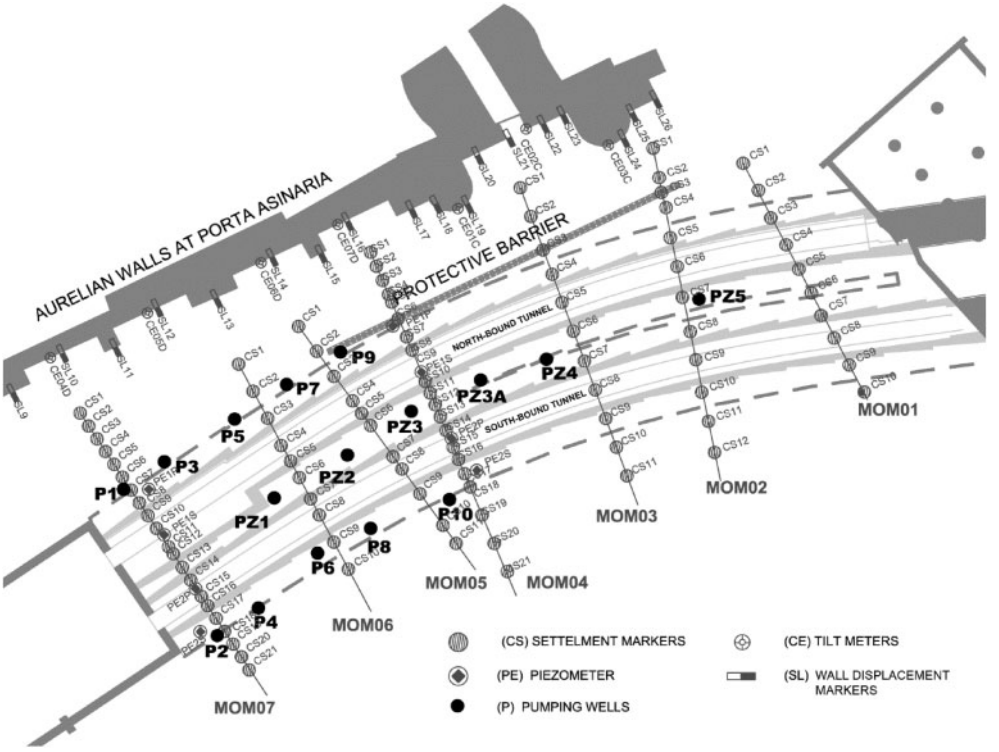

Figure 2. Plan view of the monitoring system.

To mitigate tunnelling-induced effects on the city wall, an embedded barrier made by adjacent piles was installed before tunnelling activities begun. It extends for 63 m in the zone where the North-bound tunnel is closer to the wall: 23 m and 26 m at MOM-02 and MOM-04 alignments, (Figure 2). The piles have a diameter $D = 0.8$ m, a length $L = 28$ m, and are installed at a spacing $s = 1.0$ m. The barrier runs approximately parallel to the wall with a minimum distance of about 8 m from the axis of the North-bound tunnel, about 8 m wide, and 18 m from the ancient city wall. An embedded capping beam (cross-section of $1 \times 1\text{m}^2$) connects the head of the piles. The capping beam and the piles are made of cast-in-place reinforced concrete, with a 28-day compressive strength of 32 MPa and Young's modulus of 31 GPa, while the yield strength of the rebar steel is equal to 235 MPa.

To monitor the ground movements induced by the tunnelling activities, seven arrays of instruments were set up about normal to the tunnels, named sections MOM 01-02-03-04-05-06-07. The instrumentation along the MOM alignments included settlement markers installed at ground surface and vibrating-wire piezometer cells. Arrays MOM-07 and MOM -04 were instrumented with closer displacement markers (spacing 2.5 m) and vibrating-wire piezometer cells, as well as with inclinometer and Trivec casings, the first providing horizontal displacements only, while the second measuring the three orthogonal components Δx, Δy and Δz of the displacement vectors along the

vertical measuring line, with a depth spacing of 0.5 m. The displacement markers installed at the ground surface incorporate sockets into which a removable survey plug can be screwed with good positional repeatability for manual surveying.

In this paper, reference is made to surface ground settlements measured by precision levelling only: this was performed using a digital level which can detect the height of the plane of collimation on a suitable bar-coded staff to a resolution of 0.01 mm.

Monitoring of the wall movements during the excavation activities was performed through precision levelling on displacement markers installed along the wall side facing the tunnels, about 0.5 m above the ground level, and by electric tiltmeters installed at wall mid-height to measure the out-of-plane rotation.

Ground conditions at *Porta Asinaria* are described by Fantera et al. (2016), Masini et al. (2019a–b, 2021a–b), Masini and Rampello (2021) and Rampello et al. (2019), to which reference is made for further details. Table 1 reports the strength parameters and the overconsolidation ratio as obtained from laboratory tests.

A section through the instrumented array MOM-04 is plotted in Figure 3, showing soil layering, the two tunnels, and the protective barrier. A 14 m-thick layer of made ground (MG) is first encountered, from ground surface at about +35 m asl, mainly consisting of coarse grained material, sand and gravel; recent alluvial soils of the Tiber river are found underneath, extending down to a depth of 26 m (+8.7 m asl). The alluvia are variable in grading involving slightly overconsolidated clayey silt and sandy silt (CS-SS); they overly a layer of sand and gravel of Pleistocene age (SG), with a thickness of about 14m, followed by a thick layer of stiff and overconsolidated silty clay (OSC), the blue Vatican clay of Pliocene age.

Table 1. Strength parameters and overconsolidation ratio.

Soil	γ (kN/m^3)	c' (kPa)	ϕ' (°)	OCR (−)	S_u (kPa)
Made Ground (MG)	17	5	34	1	–
Clayey silt and Sandy Silt (CS-SS)	19.5	28	27	1.25	120
Sandy Gravel (SG)	20	0.1	40	1	–
Overconsolidated Stiff Clay (OSC)	20.9	41.3	25.7	2.5	400

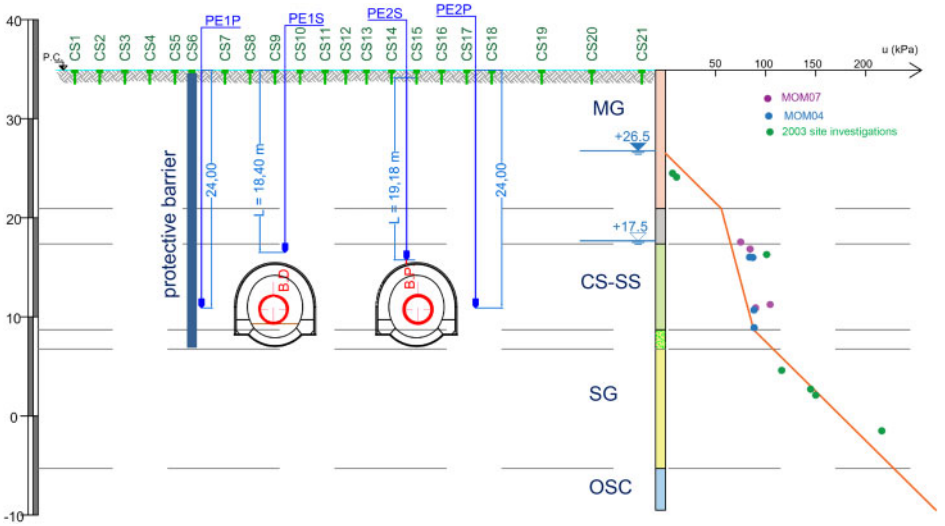

Figure 3. Transversal section through instrumented array MOM-04.

The pore water pressure regime is characterised by downwards seepage in the silty soils from the made ground, where a constant hydraulic head $H = 26.5$ m asl was measured, to the deep layer of sandy gravel, at constant head $H = 17.5$ m asl. This is a typical condition encountered along the line C of Rome underground, induced by pumping from the deep and permeable layer of sandy gravel for anthropic purposes. Tunnels excavation was carried mainly in the alluvia sandy silt whose permeability was preliminary reduced via low-pressure cement grouting.

The two tunnels connecting the multifunctional pit 3.3 to *San Giovanni* station were excavated following a three-step procedure: (i) two small-diameter tunnels ($D = 3$ m) were first excavated using a mini-slurry shield, tunnelling boring machine at a depth of about 25 m (cover to diameter ratio $C/D = 7.8$); (ii) soil improvement via low-pressure cement grouting was then carried out using t*ubes à manchettes* installed in boreholes excavated radially to the bored tunnels; (iii) tunnel construction was finally completed through conventional excavation of the main tunnels in the improved soil. Both the tunnels have a curvilinear cross-section with an average diameter of the equivalent circular cross-section $D_{eq} = 8.03$ m. At the alignment MOM-07, the initial portion of the North-bound tunnel has an enlarged cross-section with an equivalent diameter $D_{eq} = 10.3$ m.

Figure 4 shows the mini-TBM at the launching pit (Figure 4a) and at the intermediate jacking station (Figure 4b), a view from the inside of a mini-tunnel after completion of the radial injections (Figure 4c) and an intermediate stage of tunnel excavation in the improved soil (Figure 4d – primary lining installed).

At stage (ii), the *tubes à manchettes* (4 *manchettes*/m) were installed in 20 boreholes per section, drilled at a longitudinal spacing of 0.6 m: the boreholes had a diameter of 80 mm, a length of 5–7 m and a spacing of 18° in the radial direction. Soil improvement was obtained injecting first a Mistrà-type cement grout with 10–15% of bentonite content and a water-cement ratio of 2.5–3.5, and a chemical mixture of silica components in a second stage, to reduce further the permeability of the improved soil that had to be excavated during tunnelling.

Figure 4. Mini-TBM at the launching pit and at the intermediate jacking station (a-b); mini tunnel at the completion of radial injections (c); conventional tunnelling in the improved soil.

In the conventional excavation procedure, fan-like overlapping pipe umbrellas, made by 114.7 mm-diameter steel pipes, were drilled and grouted at the roof of the tunnel, parallel to the direction of advancement of the excavation face. Each roof shield consisted of 41 steel pipes, 12 m long, covering an excavation span of 8m. Full face excavation was carried out along with the installation of the primary support 1m away from the excavation face, which consists of IPN 160 steel ribs and 0.2 m-thick shotcrete. The final concrete lining, 0.8–1.0 m-thick, was installed 35 m away from the excavation face.

At the early stages of excavation of the invert of the South-bound tunnel, the first to be excavated, a local collapse involved a small portion of soil at the tunnel spring line as a result of basal heave of the improved soil. Therefore, before continuing the tunnelling activities, 16 relief wells were activated (see Figure 2), which induced an average drawdown of the hydraulic head of about 9.5 m in the layer of sandy gravel.

4 FIELD MONITORING

In this section the vertical displacements measured at ground surface by the settlement markers installed along the 6 instrumented arrays, MOM-07 to MOM-02, are discussed for each excavation stage, interpreting the transversal displacement profiles attained in plane strain conditions through the empirical relationships currently adopted in applications (e.g.: Moh et al. 1996; O'Reilly & New 1982; Peck 1969).

For evaluating the effects induced by mini-tunnelling, the reference undeformed ground surface was calculated as the average over the time of the displacement readings taken for distances of the excavation face not lower than 30 m from each instrumented section. The effects induced by radial borehole drilling were instead evaluated assuming as base-line the time average of the readings in the time interval between the end of excavation of the North-bound mini-tunnel and the start of drilling (31/03/17–27/06/17), while the reference of each section for the low-pressure grouting injections was taken considering the displacement measured about two months before the start of the injection activities.

Table 2 reports the start and end dates of each construction phase: excavations of both the small-diameter tunnels using the mini TBM was carried out in about two months (70 days), while soil improvements around the mini-tunnels took about 16 months (7 months for boreholes drilling and 9 months for grout injections). Conventional tunnelling required a much longer time, of about one year and a half for the South-bound tunnel due to some problems occurring during the excavation of the tunnel invert, while North-bound tunnel was excavated in about half year.

Typical time histories of the vertical displacements observed at the instrumented arrays are shown in Figure 5 with reference to section MOM-04 (see Figure 2), while Table 3 reports the volume per unit length described by the settlement profiles, the corresponding volume loss (mini-tunnel diameter $D = 3$ m) and the maximum observed settlements (−)/heaves (+) measured during the construction stages preliminary to excavation of the main tunnels.

Table 2. Construction stages.

construction stage		start	end
mini-tunnelling	South-bound tunnel	20/01/17	16/02/17
	North-bound tunnel	13/03/17	31/03/17
soil improvement	borehole drilling	27/06/17	22/01/18
	grouting injections	23/01/18	19/10/18
activation of relief wells		from 20/11/18	
South-bound running tunnel		18/01/19	07/07/19
North-bound running tunnel		26/04/19	21/10/19

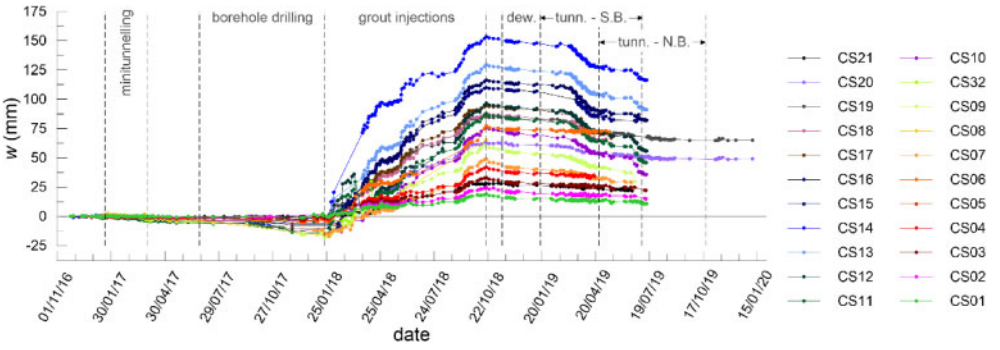

Figure 5. Time histories of the vertical displacements measured at section MOM-04.

Excavation of both the mini-tunnels induced negligible settlements, with average and maximum values $w_{ave} = -3.6$ mm and $w_{max} = -5.6$ mm, respectively, while radial boreholes drilling caused a progressive increase of the settlements as drilling activities approached the instrumented section, with $w_{ave} = -12$ mm and $w_{max} = -20.5$ mm, which are about three times higher than the corresponding values observed at the end of mini-tunnels excavation. The subsequent low-pressure grout injections caused a massive heave, with average and maximum values as high as $w_{ave} = 137.3$ mm and $w_{max} = 165.6$ mm.

Table 3. Effects induced by construction activities preliminary to excavation of main tunnels.

	tunnelling with mini-TBM			drilling of radial boreholes			low-pressure grout injections		
MOM	ΔV (m^3/m)	V_L (%)	w_{max} (mm)	ΔV (m^3/m)	V_L (%)	w_{max} (mm)	ΔV (m^3/m)	V_L (%)	w_{max} (mm)
07	0.110	0.78	–4.01	0.211	1.49	–8.43	–3.035	–21.47	95.75
06	0.202	1.43	–5.61	0.892	6.31	–20.47	–4.032	–28.52	132.7
05	0.095	0.67	–2.98	0.284	2.00	–12.92	–12.29	–86.23	141.5
04	0.099	0.70	–3.26	0.451	3.19	–13.06	–5.65	–39.96	150.0
03	0.084	0.59	–3.41	0.212	1.50	–12.33	–5.89	–41.66	165.6
02	0.062	0.44	–2.61	0.098	0.69	–4.55	–4.59	–32.47	138.4

Part of the measured heave was lost during excavation of the main tunnels, as a result of both the conventional tunnelling activities and the dewatering from the relief wells in the deep layer of sandy gravel.

Measurements provided by precision levelling during mini-tunnelling and borehole drilling are characterised by a significant scatter do not highlighting any clear difference between the volume losses computed in the presence and the absence of the barrier.

Figure 6a–b show the heave profiles induced by the grout injections carried out to improve the soil strength and reduce its permeability. Although the low pressures adopted to inject the grout, the heave measured at ground surface was not negligible in *green-field* conditions (MOM 07-06-05), being equal to about 96 mm to 140 mm, and was even higher in the sections interacting with the barrier (MOM 04-03-02), being in the range of 138 mm to 166 mm. The barrier did not produce any appreciable reduction of the ground uplift behind its location, in the portion of the soil facing the walls.

At the start of construction of the South-bound running tunnel, during the excavation of the tunnel invert, water came into the tunnel due basal heave of the improved soil, so that the excavation was

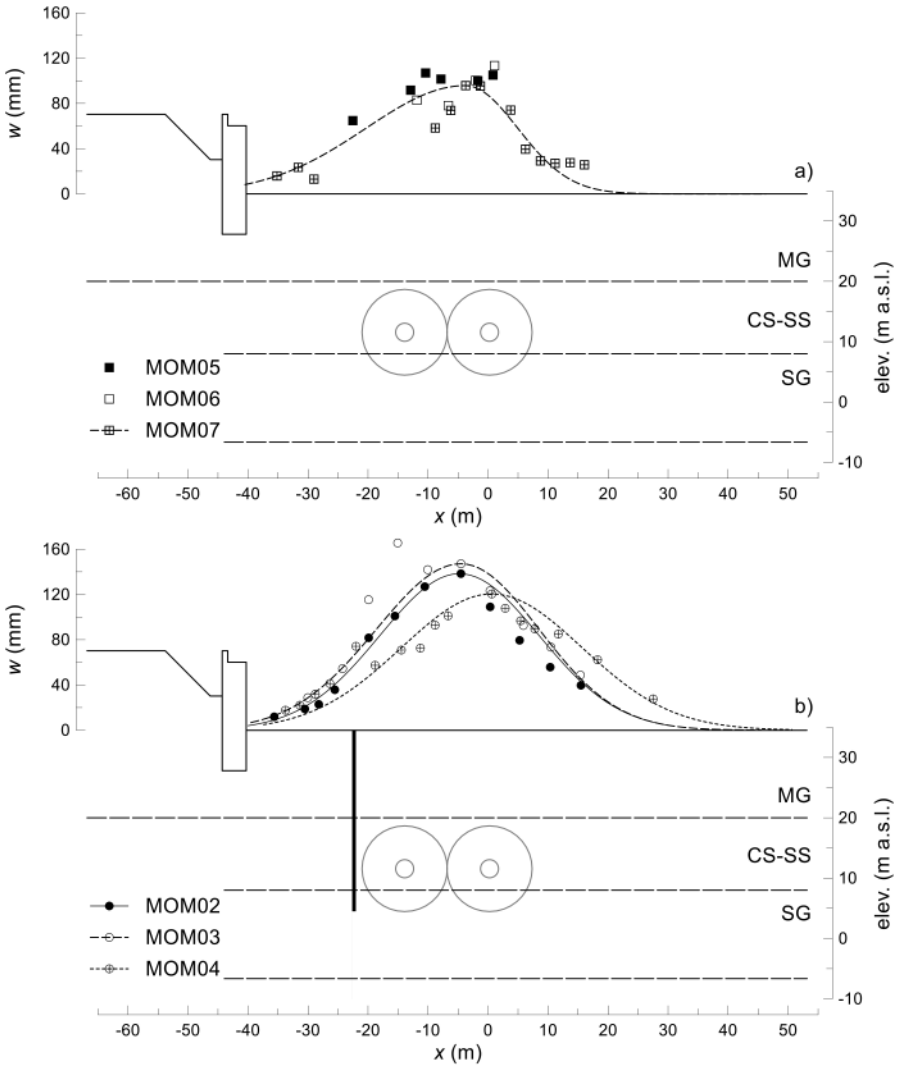

Figure 6. Settlement profiles induced by low-pressure grout injections at the *green-field* monitoring sections MON-05-06-07 (a), and in the presence of the barrier (sections MON-02-03-04) (b).

suspended while activating the pumping wells to reduce the hydraulic head at the base of the improved soil (see Figure 2). The excavation was resumed about two months later.

Pumping from the relief wells lowered the hydraulic head by about 9.5 m in the layer of sandy gravel (SG), with an increase of the effective stresses in the layer of clayey silt and the development of further settlements at ground surface.

To assess the effect of dewatering in the sandy gravel, the time needed to attain the end of consolidation in the layer of clayey silt and sandy silt (CS-SS) was evaluated using Terzaghi's theory of one-dimensional consolidation assuming a consolidation coefficient $c_v = 2 \cdot 10^{-4}$ m^2/s, and a drainage path of 12 m, evaluating an end-of-consolidation time of about 10 days. Therefore, the settlements induced at ground surface by dewatering can be assumed to be nearly fully developed before the start of tunnel excavation.

As an example, Figure 7a shows the time-history of the surface settlement measured by the settlement marker CS14 of the array MOM-07, starting from the beginning of well activation (20/11/2018).

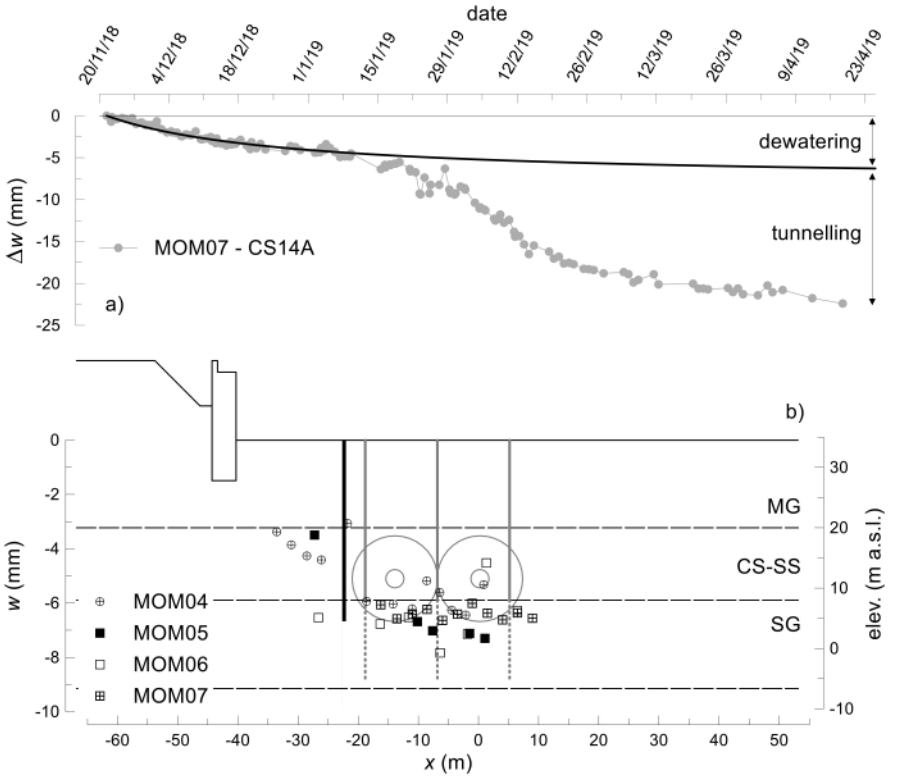

Figure 7. Time-history of the relative settlements observed during dewatering and excavation of the South-bound tunnel (a); settlements induced by the dewatering operations (b).

The first portion of the curve is characterised by a slow increase in the settlements, attributable to the consolidation process induced by dewatering, while the second presents a sharper increase associated to tunnels excavation. The first portion of the curve can be best-fitted using a hyperbole, the origin of which corresponds to the start of the pumping activities, thus estimating the final settlements induced by dewatering.

The ground surface settlements induced by lowering the pore water pressure in the sandy gravel are plotted in Figure 7b in a section transversal to the axes of the mini-tunnels. All the monitoring arrays affected by the dewatering activities exhibit similar behaviour, with a large scatter of the data and maximum settlements of –7 mm to –8 mm between the relief wells, above the two mini-tunnels.

The barrier made of adjacent piles and partially embedded in the layer of sandy gravel had, as expected, no effect in the observed settlement profiles.

Figure 8a–b show the settlement troughs induced by the excavation of both the tunnels in the green-field sections (MOM 07-06-05) and in the sections interacting with the barrier (MOM 04-03-02): the zero abscissa is referred to the axis of the South-bound tunnel.

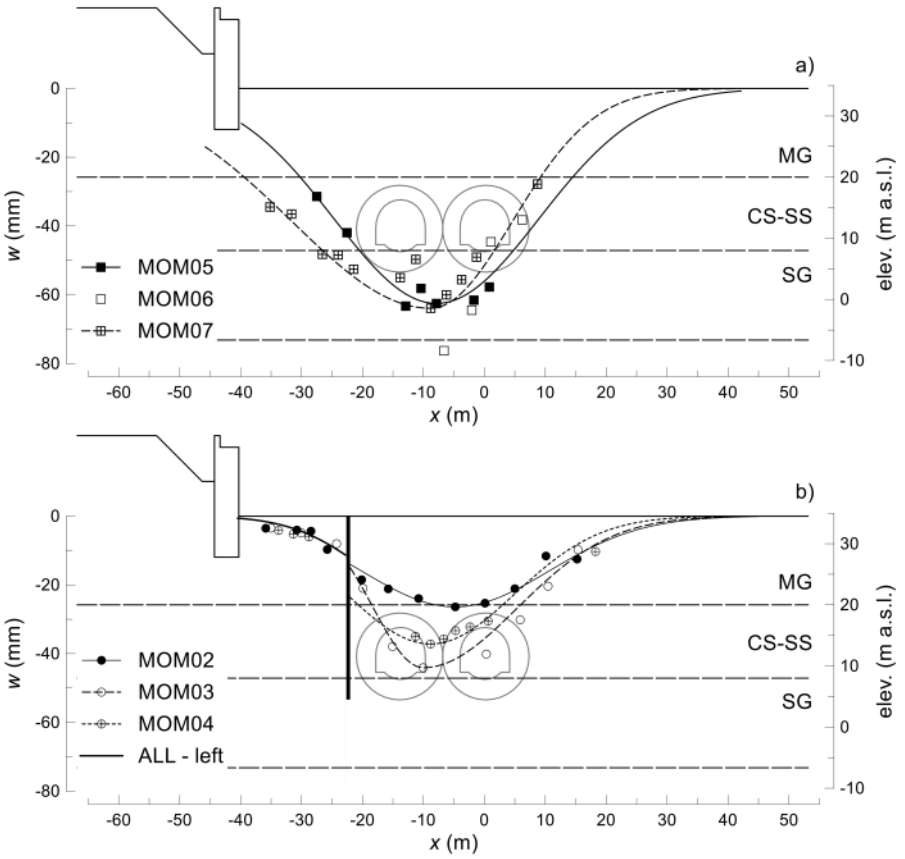

Figure 8. Settlement profiles induced by excavation of South-bound tunnel at the *green-field* monitoring sections MON-06-07 (a), and in the presence of the barrier (sections MON-04-05) (b).

The *green-field* sections show higher settlements, with maximum values of about –65 mm (Table 4), attained at about the mid plane between the tunnels. An asymmetrical settlements trough was also observed at section MOM-07, due to the larger excavated cross-section of the North-bound tunnel, so that separate best-fit Gaussian approximation of the surface settlements was carried out to the wright (+) and the left (−) of the maximum settlement, providing a trough width factor $i^{(-)} = 22.7$ m much higher than $i^{(+)} = 13.4$ m. Surface settlements evaluated at the location of the Aurelian Walls were also higher at section MOM-07, being equal to about −20 mm, if compared with the ones at section MOM-05, that are equal to about −12 mm.

For the sections interacting with the protective barrier (Figure 8b), lower settlements were measured both above the tunnels and close to the Aurelian Walls: maximum settlements above the tunnels were of about –26 mm to –44 mm (Table 4), while at the location of the Aurelian Walls, the surface settlements were not higher than –5 mm. At the wall façade a settlement reduction of 58% was obtained, while at the location of the embedded barrier the measured settlements reduced by about 72% being equal to about –43 mm in *green-field* conditions (sect. MOM-05, Figure 8a) and about –12 mm in the presence of the embedded barrier (MOM 04-03-02, Figure 8b). The efficiency of the adopted mitigation intervention is also appreciable considering the volume loss computed for green-field conditions, $V_L = 2.60\%$ (sect. MOM-05) and in the presence of the protective barrier, $V_L = 0.96\% - 1.31\%$, with an average reduction of about 56%.

It is worth mentioning that the FE interaction analyses predicted slightly lower reductions of the surface settlements at the wall and the barrier locations, equal to 41% and 66%, respectively, that were in a fair agreement with the observed reductions mentioned above, equal to 58% and 72%, respectively.

Table 4. Effects induced by tunnels excavation.

	MOM	$i^{(-)}$	$i^{(+)}$	ΔV (m^3/m)	V_L (%)	w_{max} (mm)
green-field	07	22.7	13.4	3.643	2.71	–64.0
	05	16.8	16.8	2.635	2.60	–62.6
	04	13.9	13.9	1.163	1.15	–37.2
protective barrier	03	8.2	15.5	1.327	1.31	–44.1
	02	15.4	15.4	0.969	0.96	–26.4

It is worth noting that the maximum settlements induced by dewatering plus conventional excavation of the main running tunnels (≈ -75 mm) were sensibly lower than the maximum heave induced by the grout injections carried out at low pressure from by the radial *tubes à manchettes* ($\approx$ 165 mm).

5 MOVEMENTS OF THE AURELIAN WALLS AT PORTA ASINARIA

The Aurelian Walls at *Porta Asinaria* are about parallel to the tunnels in the portion facing sections MOM-06 to MOM-03. Prior to start with the excavation activities, Metro C implemented temporary safeguarding interventions on the city wall, consisting of buttresses made by steel tube-joint structures (Figure 9) to prevent any damage eventually induced by unexpected events.

Figure 9. Temporary safeguarding interventions installed at the Aurelian Walls.

The portion of the wall facing the multifunctional pit 3.3 and the tunnels were also equipped with 10 electric tiltmeters, installed at wall mid-height to measure out-of-plane rotation, and 24 displacement markers installed at about 0.5 m above the ground surface, for monitoring the vertical

displacements of the wall (see Figure 2). Precision levelling on the displacement markers and monitoring of tiltmeters started before the tunnelling activities, on November 23rd, 2016.

The effects induced by the TBM excavation of the South-bound and North-bound mini-tunnels, as well as those induced by the radial borehole drilling to install the *tubes à manchettes* were negligible, causing displacements ≤ 2 mm, and are not discussed in the following.

To evaluate the effects of the low-pressure grout injections, the displacement measurements were referred to the start of the injections (23/01/2018), evaluating the base-line displacement profile of each section in the time interval ranging from the end of borehole drilling and the start of injections.

The maximum heave produced by the grout injections, equal to $+10.5$ mm, occurred at the displacement marker SL13, located close to the *green-field* section MOM-06, while the displacement markers located behind the protective barrier experienced substantially lower heaves, decreasing from about $+7.5$ mm (SL14–SL19) to $+3$ mm (SL22-SL26).

Tiltmeters CE 04D-05D-06D, located in front of the *green-field* sections MOM 07-06-05, provided small wall rotation towards the *Basilica di San Giovanni*, equal to about $+0.05°$, while the tiltmeters installed in the portion of the wall located behind the protective barrier, as well as those located behind the multifunctional shaft 3.3, were not substantially affected by the injection activities.

The settlements induced by conventional excavation of the South-bound and North-bound tunnels were referred to the end of the grout injections, about one month after the start of dewatering.

Figure 10 shows the isochrones of the wall settlements induced by the excavation of both tunnels. Negative abscissas in the figure refer to the displacement markers installed in the portion of the Aurelian Walls located in front of the multifunctional shaft 3.3 (SL3–SL9). The maximum settlement of the wall, equal to -12.3 mm, was measured at the location of the displacement marker SL12, located in the portion of the wall facing the *green-field* section MOM-06.

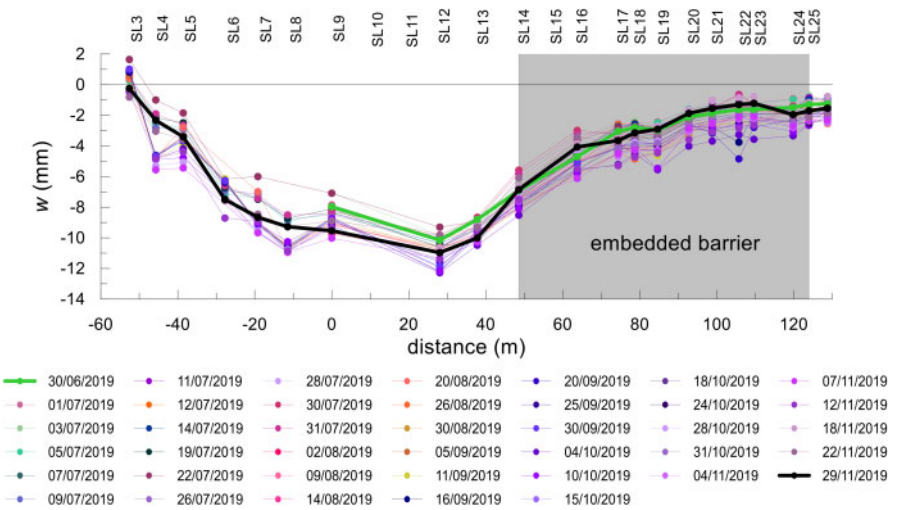

Figure 10. Settlement profiles induced by tunnelling in the Aurelian Walls.

By contrast, the wall settlements are seen to decrease behind the embedded barrier made by adjacent piles (Figure 10): moving from the displacement marker SL14, located behind the left end of the barrier, towards the displacement marker SL25, located behind its right end, the wall settlements reduce from about 7 mm (43%) to about 2 mm (84%), demonstrating the efficiency of this type of mitigation intervention. However, the reduction of wall settlement observed as *Porta Asinaria* is approached is also affected by the slight increasing distance between the North-bound tunnel and the city wall.

The maximum deflection ratios in sagging and hogging were $(\Delta_s/L_s)_{max} = 6.2 \cdot 10^{-5}$ and $(\Delta_h/L_h)_{max} = 2.7 \cdot 10^{-5}$, respectively, both resulting substantially lower than the threshold values proposed by Burland & Wroth (1974): $(\Delta_s/L_s)_{lim} = 8 \cdot 10^{-4}$ and $(\Delta_h/L_h)_{lim} = 4 \cdot 10^{-4}$.

The time histories of the out-of-plane rotations induced in the Aurelian Walls by the tunnels excavation are plotted in Figure 11.

Tiltmeters CE 01D-02D-0D3, installed in the portion of the wall facing the multifunctional shaft 3.3 show nearly constant and negligible rotations towards the excavation, of about $-0.03°$, with similar values also observed for tiltmeters CE-04D and CED-06D, installed in portion of the wall close to the transversal diaphragm wall of the shaft and the left-end of the barrier, respectively. By contrast, a maximum rotation of about $-0.08°$ was measured on the displacement marker CE-05D, installed close to the displacement marker SL12, in the portion of the wall facing the instruments array MOM-06.

Conversely, the tiltmeters installed in the portion of the wall located behind the protective barrier (CE-07D, CE 01C-02C-03C) were observed to undergo nearly zero rotations, showing once again the efficiency of the embedded barrier in reducing tunnelling effects on the ancient Aurelian Walls at *Porta Asinaria*.

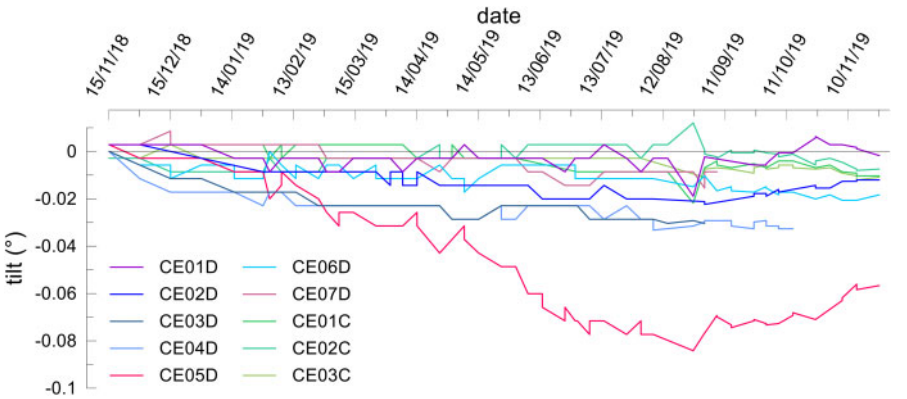

Figure 11. Time histories of the out-of-plane rotation of the Aurelian Walls at *Porta Asinaria*.

The walls were also instrumented with 11 vibrating-wire crack-meters installed over the major cracks observed in the wall façade before starting the excavation activities. Figure 12a shows the opening (−)/closure (+) measured by the crack-meters in a two-years-long time interval from 01/01/2018, before starting soil improvement via low-pressure grout injections. In the considered monitoring period, the crack-meters showed small changes in crack amplitude, with maximum values of about 0.6 mm, largely attributable to changes in the temperature. The periodic changes in crack amplitude may indeed be associated to daily and seasonal changes of temperature.

To highlight the effects of thermal excursion, Figure 12b–c show the time histories of crack opening/closure and of the changes in temperature, respectively: the data refer to a shorter time period (30/05/18–19/07/18), to make clear the strong correlation between the changes in crack-amplitude and temperature in the short (daily) and the long (seasonal) periods. Specifically, the crack-meters show amplitude changes of 0.3–0.6 mm, associated to temperature changes of about 20°C. Correlation between the changes in crack-amplitude and temperature is shown in Figure 12d for the crack-meter MG-06C, in the time period ranging from 1/1/2018 to 27/5/2019: the high computed correlation coefficient $R^2 = 0.989$ demonstrates that the observed variations in crack amplitude are mainly due to changes in the temperature. The slope of the regression line, equal to 0.017 mm/°C, provides an estimate of crack-amplitude variation of about 0.34 mm for a thermal excursion of 20°C, and of about 0.85 mm for the maximum thermal excursion monitored in the

time period 20/02/2018–31/07/2018, equal to 50.2°C: both these evaluations are consistent with the data shown in Figure 12.

It can be then concluded that the crack-meters monitored negligible effects on the main cracks present in the façade of the walls, since the changes in their amplitude are essentially attributable to thermal excursions.

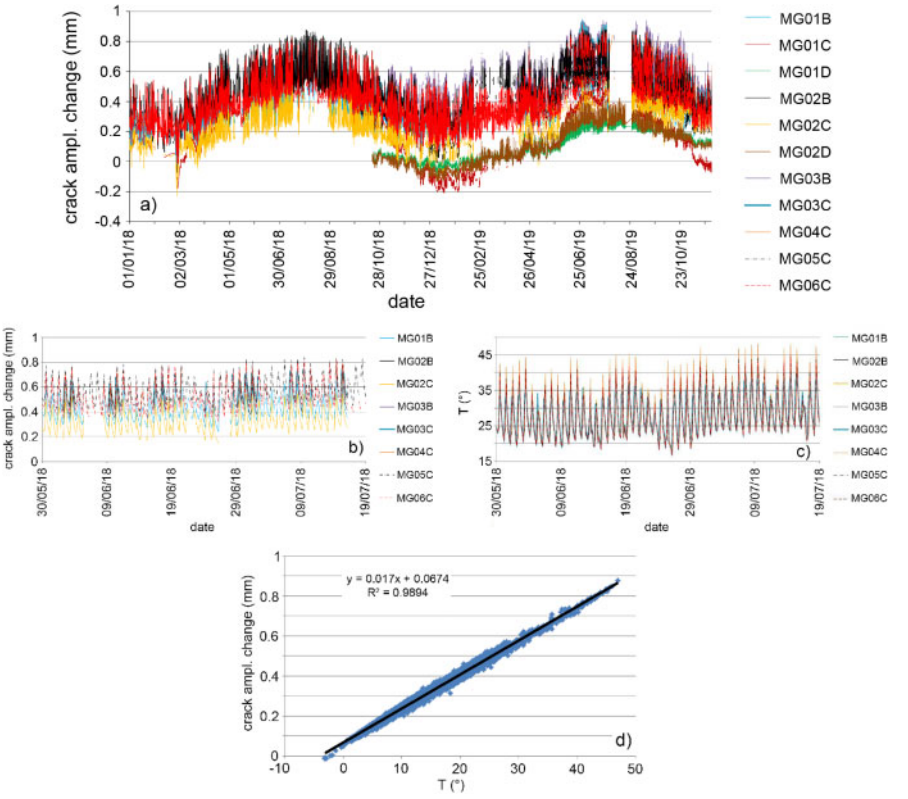

Figure 12. Measured opening (−)/closure (+) of the cracks in the Aurelian Walls.

6 CONCLUSIONS

The analysis of the monitoring data collected in a time period of about 3 years, during the excavation of two tunnels of the Line C of the Rome underground, about 140 m long, permitted to evaluate the effects induced in the Aurelian Walls at *Porta Asinaria* by the construction activities: the low-pressure grout injections preliminary carried out to improve the soil properties of the clayey silt to be excavated during tunnelling and the subsequent excavation of both running tunnels via conventional techniques.

Grout injections, though carried out under low-pressures, induced substantial heave of ground surface above the mini-tunnels, of 80 mm to 150 mm, that were seen to be larger than the maximum settlements induced by subsequent activities: dewatering by the relief wells, which induced maximum settlements of about −10 mm, and tunnels excavation, that produced surface settlement in the range −60 mm to −80 mm.

To prevent any damage in the Aurelian Walls at *Porta Asinaria*, a protective barrier of horizontal extension $L_h = 63$ m, made of adjacent piles 28 m long, partially embedded in the layer of sandy

gravel was installed about parallel to the city wall, at a distance of about 8m from the axis of the North-bound tunnel, and of about 18 m from the wall.

The barrier demonstrated to be effective in reducing the settlements induced by tunnels excavation behind its location. Indeed, at the location of the embedded barrier the measured settlements reduced by about 72%, being equal to about −43 mm in *green-field* conditions and to −12 mm in the presence of the embedded barrier. Presence of the barrier was also effective in reducing by about 56% the volume loss evaluated in the arrays interacting with it: values of $V_L = 0.96\% - 1.31\%$ were computed in the presence of the barrier, against a *green-field* volume losses $V_L = 2.60\%$.

The beneficial effects of the protective barrier were also evident for the Aurelian Walls that experiences maximum settlements of about 12 mm in the portion of the wall facing the *green-field* sections, while substantially lower values, of 3 to 7 mm, were measured in the portion of the wall located behind the barrier.

Despite the differential settlements measured along the wall development, the subsidence profile always provided maximum deflection ratios Δ/L lower than the threshold values suggested in the literature, both in sagging and hogging. Moreover, the barrier was effective in reducing the out-of-plane rotation of the wall towards the tunnels: this was equal to a maximum of about $-0.08°$ in the wall portion facing the *green-field* sections, reducing to about $-0.03°$ for the wall portion protected by the embedded barrier.

It may be concluded that the embedded barrier was effective in preventing any damage potentially induced by conventional tunnelling to the Aurelian Walls at *Porta Asinaria* and that the excavation activities were performed within the design prescriptions, without causing any detrimental effect on the ancient city wall.

ACKNOWLEDGEMENTS

The Authors are indebted to Metro C ScPA, particularly to Mr. Eliano Romani, for making available all the monitoring data.

REFERENCES

Attewell, P.B. & Woodman, J.P. 1982. Predicting the dynamics of ground settlement and its derivatives caused by tunnelling in soil. *Ground Engineering*, **15**(8), 13–22, 36.

Attewell P.B., Yeates, J. & Selby, A.R. 1986. Soil movements induced by tunnelling and their effects on pipelines and structures. Glasgow: Blakie.

Bai, Y., Yang, Z. & Jiang, Z. 2014. Key protection techniques adopted and analysis of influence on adjacent buildings due to the Bund Tunnel construction. *Tunnelling and Underground Space Technology*, **41**, 24–34.

Bilotta, E. & Taylor, R.N. 2005. Centrifuge modelling of tunnelling close to diaphragm wall. *Int. J. Phys. Model. Geotech.* **1**, 25–41.

Bilotta, E. 2008. Use of diaphragm walls to mitigate ground movements induced by tunnelling. *Géotechnique* **58** (2), 143–155.

Burghignoli, A., Callisto, L., Rampello, S., Soccodato, F.M. & Viggiani, G.M.B. 2013. The crossing of the historical centre of Rome by the new underground Line C: a study of soil structure-interaction for historical buildings. In *Geotechnics and Heritage: Case Histories*: 97–136. London: CRC Press.

Burland, J.B. & Wroth, C.P. 1974. Settlements of buildings and associated damage. *Proc. Int. Conf. on Settlements of Structures*, Cambridge, 611–654.

Di Mariano, A., Gens, A., Gesto, J.M. Schwartz, H. 2007. Ground deformation and mitigating measures associated with the excavation of the new Metro line. In *Geotechnical Engineering in Urban Environments*, Proc. of the 14th ECSMGE, Millpress Science Publisher, Rotterdam, The Netherlands, vol. **4**: 1901–1906.

Fantera, L., Rampello, S. & Masini, L. 2016. A Mitigation Technique to Reduce Ground Settlements Induced by Tunnelling Using Diaphragm Walls. *Procedia Engineering* **158**, 254–259.

Katzenbach, R., Leppla, S., Vogler, M., Seip, M. & Kurze, S. 2013. Soil-structure interaction of tunnels and superstructures during construction and service time. In: *Proc. of the 11th Int. Conf. on Modern Building Materials, Structures and Techniques*, MBMST 2013. Procedia Engineering, vol. **57**: 35–44.

Losacco N., Romani E., Viggiani G.M.B., Di Mucci G. 2019. Embedded barriers as a mitigation measure for tunnelling induced settlements: A field trial for the line C in Rome. In: *Proc. of the WTC 2019 ITA-AITES World Tunnel Congress*, Naples, Italy

Mair, R.J. & Hight, D. 1994. Compensation grouting. *World Tunnelling Subsurface Excavation* **7** (8).

Mair, R.J. 2008. 46th Rankine Lecture: Tunnelling and geotechnics: new horizons. *Géotechnique* **58** (9), 695–736.

Masini, L., Rampello, S., Viggiani, G.M.B., & Soga, K. 2012. Experimental and numeri-cal study of grout injections in silty soils. Proc. *7th International Symposium on Geotechnical Aspects of Underground Construction in Soft Ground*, Rome, 495–503.

Masini, L., S. Rampello, & K. Soga. 2014. An approach to evaluate the efficiency of compensation grouting. *J. Geotechnical and Geoenvironmental Engineering* **140** (12): 04014073.

Masini, L., Rampello, S. & Romani, E. 2019a. Performance of a deep excavation for the new Line C of Rome underground. In *Geotechnical Research for Land Protection and Development* – Proc. of CNRIG 2019 Springer Nature Switzerland AG 2020 F. Calvetti et al. (Eds.): CNRIG 2019, Lecture Notes in Civil Engineering (LNCE) **40**: 575–582.

Masini, L., Rampello, S., Carloni, S. & Romani, E. 2019b. Ground response to mini-tunnelling plus ground improvement in the historical city centre of Rome. *In Tunnels and Underground Cities: Engineering and Innovation meet Archaeology, Architecture and Art,* WTC2019, Naples 3–9 May: 5876–5885.

Masini, L., Gaudio, D., Rampello, S. & Romani, E. 2021a. Observed Performance of a Deep Excavation in the Historical Center of Rome. *Journal of Geotech. Geoenviron. Eng*., ASCE, **147**(2): 05020015.

Masini, L., Rampello, S., Fantera, L. & Romani, E. 2021b. Mitigation of tunnelling effects via pre-installed barriers: the case of Line C of Rome underground. In *Challenges and Innovations in Geomechanics*, *Proc. 16th Int. Conf. of IACMAG*, Springer Nature Switzerland AG 2021, M. Barla et al. (Eds.): IACMAG 2021, Lecture Notes in Civil Engineering (LNCE), Torino 2021, **126** (2): 197–205.

Masini, L. & Rampello, S. 2021. Predicted and observed behaviour of pre-installed barriers for the mitigation of tunnelling effects. *Tunnelling and Underground Space Technology*, 118: 104200.

Moh, Z.C., Huang, R.N. & Ju, D.H. 1996. Ground movements around tunnels in soft ground. *Proc. Int. Symp. on Geotechnical Aspects of Underground Construction in Soft Ground*, London, 725–730.

O'Reilly, M.P. & New, B.M. 1982. Settlements above tunnels in the United Kingdom – Their magnitudes and prediction. *Proc. Tunnelling '82 Symposium*, London: 173–181.

Ou C.Y. & Hsieh P.G. 2011. A simplified method for predicting ground settlement profiles induced by excavation in soft clay. *Comput. Geotech*. **38** (8): 987–997.

Peck, R. B. 1969. Deep excavation and tunnelling in soft ground. State-of-the-art-report, Mex-ico City, State of the Art Volume, *Proc. 7th Int. Conf. on Soil Mech and Found. Engng* (ICSMFE): 225–290.

Rampello, S., Callisto, L., Viggiani, G.M.B. & Soccodato, F.M. 2012. Evaluating the effects of tunnelling on historical buildings: the example of a new subway in Rome. *Geomechanics and tunnelling* **5** (3): 275–299.

Rampello, S., Fantera, L. & Masini, L. 2019. Efficiency of embedded barriers to mitigate tunnelling effects. *Tunnelling and Underground Space Technology* **89**: 109–124.